Simulation Modelling Practice and Theory 17 (2009) 1160–1169

Contents lists available at ScienceDirect

Simulation Modelling Practice and Theory

journal homepage: www.elsevier.com/locate/simpat

Design and realization of hybrid ACO-based PID and LuGre friction compensation controller for three degree-of-freedom high precision flight simulator

Haibin Duan [a,*], Senqi Liu [a], Daobo Wang [b], Xiufen Yu [c]

[a] School of Automation Science and Electrical Engineering, Beihang University, Beijing 100191, PR China
[b] College of Automation Engineering, Nanjing University of Aeronautics and Astronautics, Nanjing 210016, PR China
[c] Center for Space Science and Applied Research, Chinese Academy of Sciences, Beijing 100190, PR China

ARTICLE INFO

Article history:
Received 24 April 2006
Received in revised form 15 April 2009
Accepted 16 April 2009
Available online 3 May 2009

Keywords:
Ant Colony Optimization (ACO)
Proportional–Integral–Derivative (PID)
LuGre friction
Three degree-of-freedom (3-DOF)
High precision flight simulator
Modularization
Industrial Personal Computer (IPC)

ABSTRACT

Three degree-of-freedom (3-DOF) high precision flight simulator is a type of key hardware-in-loop equipment in the fields of aeronautics and astronautics. The conventional Proportional–Integral–Derivative (PID) is a widely used industrial controller that uses a combination of proportional, integral and derivative action on the control error to form the output of the controller. It is well known that the undesired phenomena caused by friction can lead to overall flight simulator performance degradation or instability. This paper presents a novel kind of hybrid Ant Colony Optimization (ACO)-based PID and LuGre friction compensation controller for 3-DOF high precision flight simulator. On the basis of introduction of the basic principles of ACO, the controlling scheme design for the 3-DOF high precision flight simulator is presented. Based on the popular LuGre friction model, a novel nonlinear friction compensation controller for 3-DOF high precision flight simulator is also developed. The proposed Lyapunov function proves the robust global convergence of the tracking error. The parameters tuning of PID can be summed up as the typical continual spatial optimization problem, grid-based searching strategy is adopted in the improved ACO algorithm, and self-adaptive control strategy for the pheromone decay parameter is also adopted. Modularization design is adopted in the 3-DOF high precision flight simulator. This software can process the position and status signals, and display them on the friendly interface. Double buffer mechanism is adopted in the communication protocol between lower Industrial Personal Computer (IPC) and upper IPC. The series experimental results have verified the feasibility and effectiveness of the proposed hybrid ACO-based PID and LuGre friction compensation controller.

© 2009 Elsevier B.V. All rights reserved.

1. Introduction

Three degree-of-freedom (3-DOF) high precision flight simulator is a type of key hardware-in-loop equipment in the fields of aeronautics and astronautics. It could simulate the dynamic characteristics and various flying postures [1,2]. The performance of flight simulator has direct effects on the reality and credibility of simulation experiments.

The conventional Proportional–Integral–Derivative (PID) is a widely used industrial controller that uses a combination of proportional, integral and derivative action on the control error to form the output of the controller. Due to its simple structure and effectiveness, this technology has been being the mainstay for so long among practicing engineers. After the three

* Corresponding author. Tel.: +86 10 82317318; fax: +86 10 82317305.
E-mail address: hbduan@buaa.edu.cn (H. Duan).

1569-190X/$ - see front matter © 2009 Elsevier B.V. All rights reserved.
doi:10.1016/j.simpat.2009.04.006

parameters have been tuned or chosen in a certain way, control parameters of a standard PID are kept fixed during control process. There are many tuning techniques based on several methods. These methods can be classified as: (1) empirical methods such as the Ziegler–Nichols (ZN) method [3] and the Internal Model Control (IMC) [3], (2) analytical methods such as root locus based techniques [3], (3) methods based on optimization such as the iterative feedback tuning (IFT) [4] and genetic algorithm tuning technique [5]. In this work, an Ant Colony Optimization (ACO)-based PID parameters tuning strategy was presented, this approach can alleviate some of the difficulties by fusing a priori information into the PID controller design.

In 3-DOF high precision flight simulator, friction causes many undesired phenomena such as tracking errors, limit cycles, and the undesired stick-slip motion of friction can lead to overall system performance degradation or instability [6]. Several properties observed in high precision flight simulator with friction cannot be explained by static models because the internal dynamics of friction are not considered. Several models, including both static and dynamic friction, have been proposed in the last few years [7]. While the most used is the LuGre friction model and its modifications. All the static and dynamic characteristics of friction are captured by the LuGre friction model. LuGre friction model can describe arbitrary friction characteristics of high precision flight simulator.

In this paper, we present a novel kind of hybrid ACO-based PID and LuGre friction compensation controller for 3-DOF high precision flight simulator. The rest of this paper is organized as follows: In Section 2, we introduce the basic principles of ACO, followed by the controlling scheme design for the 3-DOF high precision flight simulator in Section 3. Then, Section 4 presents an improved ACO approach to the PID controller for the 3-DOF high precision flight simulator. Subsequently, hardware and software design are presented in Sections 5 and 6 in detail. Section 7 gives the experimental results to verify the performance the whole control system of the flight simulator with the hybrid ACO-based PID and LuGre friction compensation controller. Our concluding remarks and future work are contained in Section 8.

2. Principles of ACO

ACO algorithm is a meta-heuristic algorithm for the approximate solution of combinatorial optimization problems that has been inspired by the foraging behavior of real ant colonies [8–11]. In ACO algorithm, the computational resources are allocated to a set of relatively simple agents that exploit a form of indirect communication mediated by the environment to construct solutions to the finding the shortest path from ant nest to a considered problem. Real ants are capable of food source, because, while walking, ants deposit pheromone on the ground, and real ants have a probabilistic preference for paths with larger amount of pheromone. Fig. 1 shows the principle that ants exploit pheromone to establish shortest path from a nest to a food source and back.

In Fig. 1, the point A is a nest, the point E is a food source, the point B or the point C is a path-crotch, the line EF is an obstacle, and d is the distance between two points. Because of barrier EF, the ants, which comes out of nest A or go back from the food source D, can reach their destination only via E or F. Suppose all ants go there and back between A and D at a speed of 1 unit length per unit time, and there are 50 ants per unit time from A and D to D and A to decide whether to turn left or right at B and C(shown as in Fig. 1a), respectively. At first, they choose randomly (25 left and 25 right separately, shown as in Fig. 1b) for there are not any pheromones on the ways. After 1 unit time, 50 ants have passed through the shorter path BFC and deposit pheromone on the ground, which only 25 ants have done through the longer path BEC (length double BFC). Therefore, the amount of pheromone on BFC is two times as much as on BEC. Then, there again are 50 ants to choose path at B and C, respectively. Since the amount of pheromone on BFC is different from BEC, the path choice of the ants is influenced by it and is roughly proportional to it. Therefore, about 40 ants turn to direction F and the other 10 ants turn to E (shown as in Fig. 1c), and the outcome is that more pheromone deposits on shorter path BFC. As time goes on and the process repeats, the pheromone amount of the shorter path accumulates faster, and more ants choose this path. This process is thus characterized by a positive feedback loop, where the probability with which an ant chooses a path increases with the number of ants that previously chose the same path. With the above positive feedback mechanism, all ants will choose the shorter path in the end.

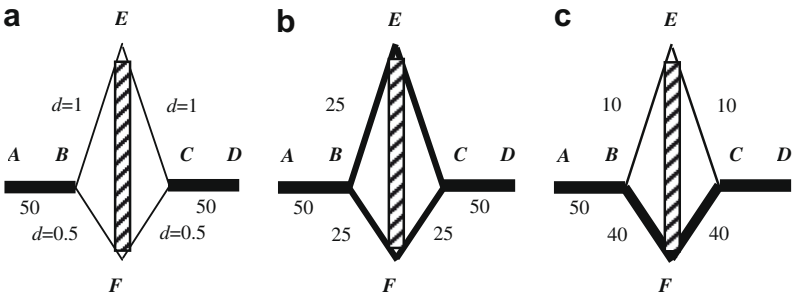

Fig. 1. Diagram of ACO algorithm principle.

3. Controlling scheme for 3-DOF high precision flight simulator

Closed-loop PID control scheme is adopted in the 3-DOF high precision flight simulator. Derivative action helps to predict the error and the proportional derivative controller uses the derivative action to improve closed-loop stability. The integral action can increase the control signal if there is a small positive error. The 3-DOF high precision flight simulator with the hybrid ACO-based PID and LuGre friction compensation controller is presented by the architecture in Fig. 2.

3.1. Conventional PID controller

The control law of the PID controller is presented as follows [12]:

$$u(n) = K_p\left(e(n) + \frac{1}{T_i}\sum_{k=0}^{n} e(k)T + T_d\frac{e(n)-e(n-1)}{T}\right) \tag{1}$$

where $u(n)$ is the current control variable, $e(n)$ is the current error, K_p is the proportional constant, T_i is the integral time constant, T_d is the derivation time constant, and T is the step of simulation.

Eq. (1) is generally named as the position PID control law, and there is another type of PID, incremental PID [13], which can be expressed as follows:

$$\Delta u(n) = K_p\{[e(n)-e(n-1)] + \frac{T}{T_i}e(n) + \frac{T_d}{T}[e(n)-2e(n-1)+e(n-2)]\} \tag{2}$$

It is clear that there are only three parameters, which are K_p, T_i and T_d, needed to be identified in the conventional PID controller.

3.2. Performance index

The performance index of smallest Integrated Time Absolute Error (ITAE) was first proposed by Graham and Lathrop. The ITAE seldom considers the big initial error, and emphasizes the overshoot and the control time. ITAE reflects the rapidity and accuracy of the control system, and is widely used in the field of control technology [12]. The equation of ITAE is as follows.

$$J_{\mathrm{ITAE}} = \int t|e(t)|dt = \min \tag{3}$$

Discretize the above equation, can result in the difference equation as follows:

$$J_{\mathrm{ITAE}} = \sum_{k=0}^{N} |e(kT)|kT = \min \tag{4}$$

where N denotes the nodes number of real-time simulation.

3.3. LuGre friction model for high precision flight simulator

The 3-DOF high precision flight simulator mechanism under study is modeled as a simple mass system with dynamic friction, described by

$$u - F = J\frac{d^2\theta}{dt^2} \tag{5}$$

where u is the control force, J is the effective inertia of the 3-DOF high precision flight simulator, θ is the angular position, and F is the friction force, which is described by the LuGre friction model [14,15] as following

$$F = \sigma_0 z + \sigma_1\frac{dz}{dt} + \alpha\frac{d\theta}{dt} \tag{6}$$

$$\frac{dz}{dt} = \frac{d\theta}{dt} - \frac{\sigma_0\left|\frac{d\theta}{dt}\right|}{h\left(\frac{d\theta}{dt}\right)}z \tag{7}$$

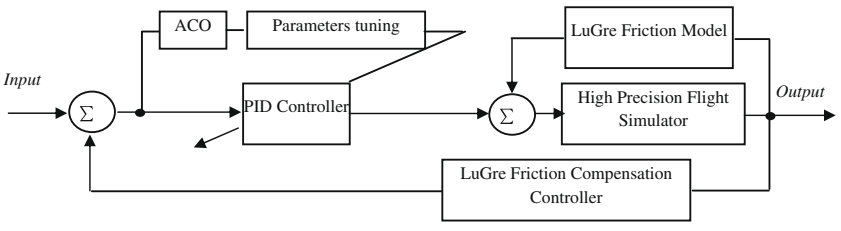

Fig. 2. Architecture of 3-DOF high precision flight simulator with ACO-based PID and LuGre friction compensation controller.

where z denotes the average deflection of the bristles, σ_0 is the stiffness of bristles,σ_1 is the damping coefficient, α is the viscous coefficient, and the nonlinear friction characteristic function $h(\frac{d\theta}{dt})$ is a finite positive function. The typical parameterization of $h(\frac{d\theta}{dt})$ to characterize the Stribeck effect is given as following.

$$h\left(\frac{d\theta}{dt}\right) = f_c + (f_s - f_c)e^{-\left(\frac{d\theta/dt}{d\theta_s/dt}\right)^2} \tag{8}$$

where f_c is the Coulomb friction level, f_s is the level of the stiction force and $\frac{d\theta_s}{dt}$ is the constant stribeck velocity.

4. LuGre friction compensation controller for high precision flight simulator

Let us insert Eqs. (6) and (7) into Eq. (5), the flight simulator model Eq. (5) can be re-written as:

$$J\frac{d^2\theta}{dt^2} = u - F = u - \sigma_0 z - \sigma_1\frac{dz}{dt} - \alpha\frac{d\theta}{dt} = u - \sigma_0 z - \sigma_1\left(\frac{d\theta}{dt} - \frac{\sigma_0\left|\frac{d\theta}{dt}\right|}{h\left(\frac{d\theta}{dt}\right)}z\right) - \alpha\frac{d\theta}{dt} = u - \sigma_0 z - \frac{\sigma_0\sigma_1\left|\frac{d\theta}{dt}\right|}{h\left(\frac{d\theta}{dt}\right)}z - (\sigma_1+\alpha)\frac{d\theta}{dt} \tag{9}$$

Suppose the tracking error $e = \frac{d\theta}{dt} - \frac{d\theta_{ref}}{dt}$, whose derivative could be calculated as:

$$J\frac{de}{dt} = u - \sigma_0 z - \frac{\sigma_0\sigma_1\left|\frac{d\theta}{dt}\right|}{h\left(\frac{d\theta}{dt}\right)}z - (\sigma_1+\alpha)\frac{d\theta}{dt} - J\frac{d\theta_{ref}}{dt} \tag{10}$$

$$\frac{d\hat{z}}{dt} = \frac{d\theta}{dt} - \frac{\sigma_0\sigma_1\left|\frac{d\theta}{dt}\right|}{h\left(\frac{d\theta}{dt}\right)}\hat{z} + t \tag{11}$$

where $\hat{z}$ is the estimate for friction state z, and t is observer dynamic term.

$$\frac{dz_e}{dt} = -\frac{\sigma_0\sigma_1\left|\frac{d\theta}{dt}\right|}{h\left(\frac{d\theta}{dt}\right)}z_e - t \tag{12}$$

where $z_e = z - \hat{z}$, we choose the control u as:

$$u = -ce + \hat{\sigma}_0 z + \frac{\hat{\sigma}_0\hat{\sigma}_1\left|\frac{d\theta}{dt}\right|}{h\left(\frac{d\theta}{dt}\right)}\hat{z} + (\hat{\sigma}_1+\hat{\alpha})\frac{d\theta}{dt} + J\frac{d\theta_{ref}}{dt} \tag{13}$$

where $\hat{\sigma}_0, \hat{\sigma}_1, \hat{\alpha}, \hat{z}$ are the corresponding parameter estimates in Eq. (10), and c is a positive constant parameter. Inserting Eq. (13) into Eq. (10), we could have:

$$\begin{aligned}
J\frac{de}{dt} &= -ce + \hat{\sigma}_0 z + \frac{\hat{\sigma}_0\hat{\sigma}_1\left|\frac{d\theta}{dt}\right|}{h\left(\frac{d\theta}{dt}\right)}\hat{z} + (\hat{\sigma}_1+\hat{\alpha})\frac{d\theta}{dt} + J\frac{d\theta_{ref}}{dt} - \sigma_0 z - \frac{\sigma_0\sigma_1\left|\frac{d\theta}{dt}\right|}{h\left(\frac{d\theta}{dt}\right)}z - (\sigma_1+\alpha)\frac{d\theta}{dt} - J\frac{d\theta_{ref}}{dt} \\
&= -ce + \hat{\sigma}_0 z + \frac{\hat{\sigma}_0\hat{\sigma}_1\left|\frac{d\theta}{dt}\right|}{h\left(\frac{d\theta}{dt}\right)}\hat{z} + (\hat{\sigma}_1+\hat{\alpha})\frac{d\theta}{dt} - \sigma_0 z - \frac{\sigma_0\sigma_1\left|\frac{d\theta}{dt}\right|}{h\left(\frac{d\theta}{dt}\right)}z - (\sigma_1+\alpha)\frac{d\theta}{dt} \\
&= -ce - (\sigma_0 - \hat{\sigma}_0)z - [(\sigma_1 - \hat{\sigma}_1) + (\alpha - \hat{\alpha})]\frac{d\theta}{dt} - (\sigma_0\sigma_1 z - \hat{\sigma}_0\hat{\sigma}_1\hat{z})\frac{\left|\frac{d\theta}{dt}\right|}{h\left(\frac{d\theta}{dt}\right)} \\
&= -ce - \Delta\sigma_0 z - [\Delta\sigma_1 + \Delta\alpha]\frac{d\theta}{dt} - \Delta z_\sigma\frac{\hat{\sigma}_0\hat{\sigma}_1\left|\frac{d\theta}{dt}\right|}{h\left(\frac{d\theta}{dt}\right)}
\end{aligned} \tag{14}$$

where $\Delta\sigma_0 = \sigma_0 - \hat{\sigma}_0, \Delta\sigma_1 = \sigma_1 - \hat{\sigma}_1, \Delta\alpha = \alpha - \hat{\alpha}, \Delta z_\sigma = \sigma_0\sigma_1 z - \hat{\sigma}_0\hat{\sigma}_1\hat{z}$, they are unknown parameter estimate errors.

Here, we choose the Lyapunov function for the close-loop flight simulator as:

$$V = \frac{1}{2}Je^2 + \frac{1}{2\zeta_0}\Delta\sigma_0^2 + \frac{1}{2\zeta_1}\Delta\sigma_1^2 + \frac{1}{2\zeta_2}\Delta\alpha^2 + \frac{1}{2\zeta_3}\Delta z_\sigma^2 \tag{15}$$

where $\zeta_0, \zeta_1, \zeta_2, \zeta_3$ are positive constant parameters. Then, the derivative of the Lyapunov function is:

$$\begin{aligned}
\frac{dV}{dt} &= Je\frac{de}{dt} + \frac{1}{\zeta_0}\frac{\Delta\sigma_0 d(\Delta\sigma_0)}{dt} + \frac{1}{\zeta_1}\frac{\Delta\sigma_1 d(\Delta\sigma_1)}{dt} + \frac{1}{\zeta_2}\frac{\Delta\alpha d(\Delta\alpha)}{dt} + \frac{1}{\zeta_3}\frac{\Delta z_\sigma d(\Delta z_\sigma)}{dt} \\
&= e\left(-ce - \Delta\sigma_0 z - [\Delta\sigma_1 + \Delta\alpha]\frac{d\theta}{dt} - \Delta z_\sigma\frac{\hat{\sigma}_0\hat{\sigma}_1\left|\frac{d\theta}{dt}\right|}{h\left(\frac{d\theta}{dt}\right)}\right) + \frac{1}{\zeta_0}\frac{\Delta\sigma_0 d(\Delta\sigma_0)}{dt} + \frac{1}{\zeta_1}\frac{\Delta\sigma_1 d(\Delta\sigma_1)}{dt} \\
&\quad + \frac{1}{\zeta_2}\frac{\Delta\alpha d(\Delta\alpha)}{dt} + \frac{1}{\zeta_3}\frac{\Delta z_\sigma d(\Delta z_\sigma)}{dt} \\
&= -ce^2 - \Delta\sigma_0\left(z - \frac{1}{\zeta_0}\frac{d(\Delta\sigma_0)}{dt}\right) - \Delta\sigma_1\left(\frac{d\theta}{dt} - \frac{1}{\zeta_1}\frac{d(\Delta\sigma_1)}{dt}\right) - \Delta\alpha\left(\frac{d\theta}{dt} - \frac{1}{\zeta_2}\frac{d(\Delta\alpha)}{dt}\right) - \Delta z_\sigma\left(\frac{\hat{\sigma}_0\hat{\sigma}_1\left|\frac{d\theta}{dt}\right|}{h\left(\frac{d\theta}{dt}\right)} - \frac{1}{\zeta_3}\frac{d(\Delta z_\sigma)}{dt}\right) \\
&\leqslant -ce^2
\end{aligned} \tag{16}$$

5. ACO approach to PID controller for high precision flight simulator

The parameters tuning of the conventional PID can be summed up as the typical continual spatial optimization problem [11], and the general method of solving continual space optimization question using the grid-based ACO algorithm is generalized as follows.

Firstly, we may estimate the optimal solution the scope according to the problem nature, the estimated value scope of the variable can be described as $x_{jlower} \leqslant x_j \leqslant x_{jupper} (j = 1, 2, 3, \ldots, n)$. Secondly, we can divide the grids in the variable region, and the spatial grid corresponds to a condition. The ants move between different grid points, and leave different pheromone amount according to various mesh points goal function value, which can influence next batch of ants' travel direction [16–18]. After periods of time, the pheromone amount corresponding to the neighboring point objective function value is quite big. The mesh point with biggest pheromone amount could be found according to the pheromone amount. The variable scope is minimized, and the ant colony move around this point. This iteration process goes on until a certain termination condition: a certain number of iterations have been achieved; a fixed amount of CPU time has elapsed; or solution quality has been achieved.

Suppose the variable is decomposed into n parts, therefore the n variables composed the decision problem with n grades. There are $N + 1$ mesh points in each grade, and there are $(N + 1) \times n$ mesh points from grade one to grade n. By this way, a solution in the solution space is formulated. The above process can be illustrated in Fig. 3.

In Fig. 3, the state space shows the condition is (3,4, 2,…,1), and the corresponding solution is as follows

$$(x_1, x_2, x_3, \ldots, x_n) = \left(x_{1lower} + \frac{x_{1upper} - x_{1lower}}{N} \times 3, x_{2lower} + \frac{x_{2upper} - x_{2lower}}{N} \times 4, x_{3lower} + \frac{x_{3upper} - x_{3lower}}{N} \times 2, \ldots, x_{nlower} + \frac{x_{nupper} - x_{nlower}}{N} \times 1\right) \tag{17}$$

Let m is the number of the whole ant colony, and m ants are scattered randomly on the mesh nodes. In discrete time steps, all ants select their next mesh node then simultaneously move to their next node. For each ant l, we can define the appraisal function value as the difference between J_i and J_j, which can be shown as follows

$$\Delta J_{ij} = J_i - J_j, \quad \forall\, i, j \tag{18}$$

Ants deposit pheromone on each edge they visit to indicate the utility of these edges. The accumulated strength of pheromone on edge (i,j) is denoted by τ_{ij}. We assume that an real ant l located at node i chooses its next node j by applying Eq. (19), which is also called state transition rule

$$P_{ij} = \begin{cases} \frac{[\tau_{ij}]^{\alpha}[\Delta J_{ij}]^{\beta}}{\sum_{r \in allowed_l} [\tau_{ir}]^{\alpha}[\Delta J_{ir}]^{\beta}}, & \text{if } j \in allowed_l \\ 0, \quad \text{otherwise} \end{cases} \tag{19}$$

where $allowed_l$ denotes the set of mesh points available for ant l, α is the pheromone heuristic parameter, β weighs the relative importance of the heuristic value. If $\beta = 0$ only pheromone amplification will occur and the distance between nodes has no direct influence on the choice.

We may spread the ants in the spatial mesh grids according to the stochastic principle, and record the elitist ant which has the best objective function value. Then, we can move each ant according to Eq. (19). Neighbor search mechanism is adopted in the search process, e.g. when $\Delta J_{ij} > 0$, the ant l migrate from neighborhood i to neighborhood j according to Eq. (19). When $\Delta J_{ij} \leqslant 0$, the ant l will carry on neighborhood search. In this way, a better solution can be found.

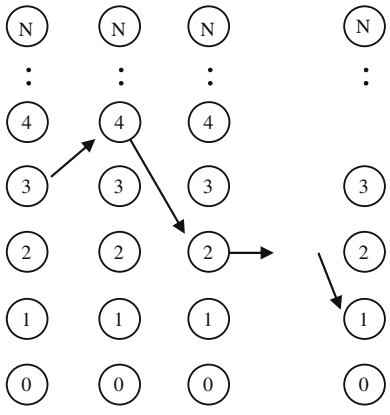

Fig. 3. Schematic figure of state space solution.

Once all ants have constructed a tour, global updating of the pheromone takes place. Here, we use elitist strategy: edges that compose the best solution are rewarded with a relatively large increase in their pheromone level. This is expressed in Eq. (20).

$$\begin{cases} \tau_{ijNew} = (1-\rho)\tau_{ij} + \Delta\tau_{ij} \\ \Delta\tau_{ij} = \sum_{l=1}^{m} \Delta\tau_{ij}^{l} \end{cases} \tag{20}$$

where ρ is the pheromone decay parameter, and $\rho \subset (0,1)$. $\Delta\tau_{ij}^{l}$ is used to reinforce the pheromone on the edge (i,j), which can be calculated by using Eq. (21).

$$\Delta\tau_{ij}^{l} = \begin{cases} \frac{Q}{J_l}, & \text{if ant } l \text{ transverse edge } (i,j) \\ 0, & \text{otherwise} \end{cases} \tag{21}$$

where Q is a constant, J_l is the objective function value of ant l in this cycle.

The bigger the parameter ρ, the bigger the iteration time N_C, and the convergence speed of the grid-based ACO algorithm will become slow. Otherwise, although the convergence speed become fast, but the calculation result is easy to fall into local best. Therefore, in order to enhance the resolution efficiency of the grid-based ACO algorithm, self-adaptive control strategy for the parameter ρ is adopted [19], this strategy can be illustrated by Eq. (22).

$$\rho(t+1) = \begin{cases} 0.9 \cdot \rho(t), & \text{if } 0.9 \cdot \rho(t) > \rho_{\min} \\ \rho_{\min}, & \text{otherwise} \end{cases} \tag{22}$$

where 0.9 is the pre-determined evaporation restraint coefficient, $\rho_{\min}$ denotes lower limit of the pheromone decay parameter.

6. Hardware design for high precision flight simulator

The dynamic behaviors of 3-DOF high precision flight simulator are mainly determined by the body dynamics of flight simulator, electric-driven actuating system, and all unpredictable disturbances.

This controller could be decomposed into three controlling feedback loops: current feedback loop, rate feedback loop and position feedback loop [20]. The current feedback loop can effectively enhance the response speed. In order to avoid mechanical failure or system malfunctioning, it is essential in all engineering situations to safeguard against the occurrence of large initial transient overshoots. The suppression of these overshoots must not, in general, be at the expense of the system accuracy. Therefore, it becomes necessary in this design to introduce additional control action to prevent this. An action of rate feedback can solve this problem effectively. Photo-electric angular encoder is the main part of position feedback loop, which has high feedback precision. The Industrial Personal Computer(IPC) is the key processing unit in the control system, and the

Fig. 4. The body structure of a type of 3-DOF high precision flight simulator.

hybrid ACO-based PID and LuGre Friction Compensation are conducted in this unit. Fig. 4 shows the body structure of the 3-DOF high precision flight simulator considered in this paper, the whole structure is designed to be axis-symmetric. Fig. 5 is a photograph of the control system of the 3-DOF high precision flight simulator.

7. Software design for high precision flight simulator

Modularization design is adopted in the 3-DOF high precision flight simulator [20]. This software can process the position and status signals, and display them on the friendly interface. The following Fig. 6 demonstrates the modularization design scheme for the developed 3-DOF high precision flight simulator software system.

From Fig. 6, it is clear that the general software system including three modes: standard function, velocity mode and simulation mode. The standard function is used to verify the characteristics of the developed high precision flight simulator by using standard signals, such as sinusoidal signals, cosinusoidal signals or triangular signals. The velocity mode is used to test the velocity characteristics of the developed high precision flight simulator. The simulation mode is used to conduct the hardware-in-loop experiments under various command signals, and this mode is realized by upper IPC and lower IPC. The upper IPC software is mainly designed for status monitoring, data processing, system analysis and integration, it can also provide standard or nonstandard simulation signals. The lower IPC software is the direct control module, which is mainly designed for position data acquisition, control law solution and communicate with upper IPC. The proposed hybrid ACO-based PID and LuGre friction compensation controller is also embedded to this module. Fig. 7 shows the lower IPC software interface for the 3-DOF high precision flight simulator. This software interface can show the running status of the whole 3-DOF high precision flight simulator, and the user can also choose different mode by pressing the corresponding buttons in this interface.

Double buffer mechanism is adopted in the communication protocol between lower IPC and upper IPC. The data to be sent is stored in second buffer firstly. If the first buffer is empty, then the data is sent to the first buffer, and the data in the first buffer will be sent to FIFO registers immediately. Otherwise, the data will be kept in the first buffer until the second buffer is empty.

8. Experimental results

Series experiments have been performed to investigate the performance of the proposed hybrid ACO-based PID and LuGre friction compensation controller for 3-DOF high precision flight simulator. We choose $\zeta_0 = 8, \zeta_1 = 6,$

Fig. 5. The control system of the 3-DOF high precision flight simulator.

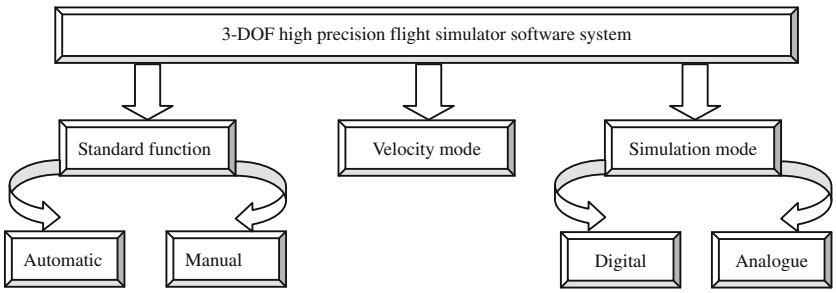

Fig. 6. Modularization design for the 3-DOF high precision flight simulator software system.

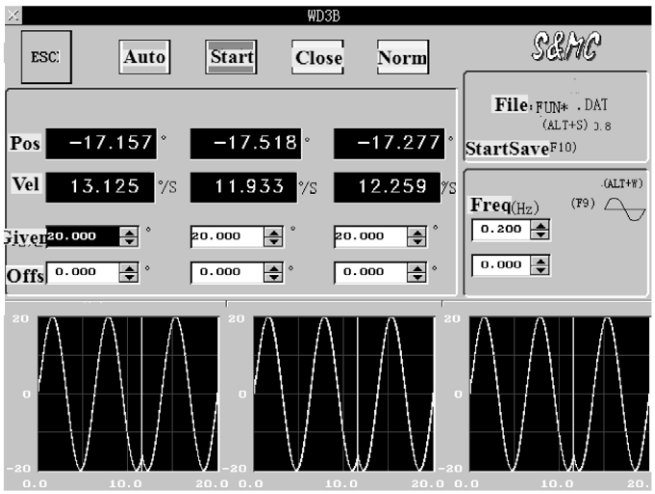

Fig. 7. The lower IPC software interface for the 3-DOF high precision flight simulator.

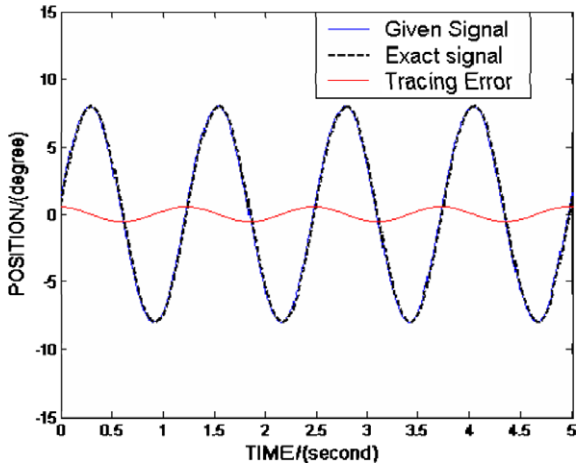

Fig. 8. Response curve of 3-DOF high precision flight simulator with standard sinusoid input signal.

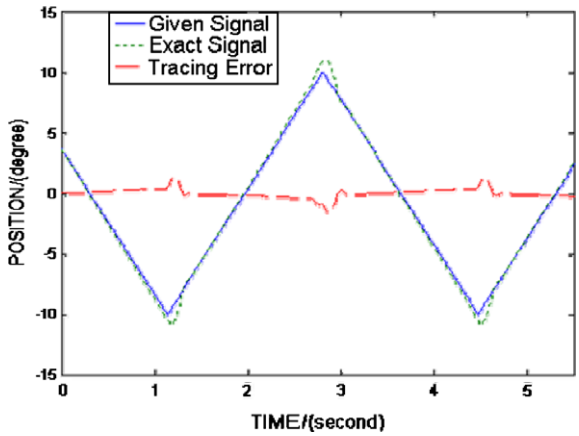

Fig. 9. Response curve of 3-DOF high precision flight simulator with standard triangle input signal.

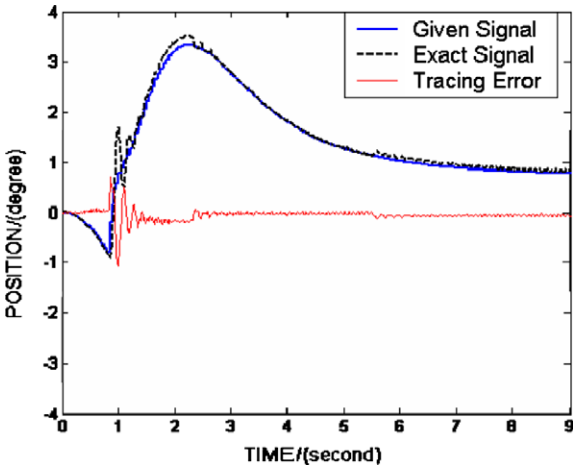

Fig. 10. Response curve of 3-DOF high precision flight simulator with nonstandard input signal.

$\zeta_2 = 8, \zeta_3 = 7, T = 0.0008$ s. The obtained average optimal solution values for the conventional PID controller are: $K_p = 1.692, T_i = 0.774, T_d = 0.351$.

In Fig. 8, the given signal is standard sinusoid wave: $\theta = 8sin(1.6\pi t)$. In Fig. 9, the given signal is standard triangle wave with 0.3 Hz and 10.0°. While in Fig. 10, the given signal is nonstandard signal.

From Figs. 8–10, we can see that the response curve of the 3-DOF high precision flight simulator with ACO-based PID and LuGre friction compensation controller can achieve high precision and fast tracking response.

9. Conclusions and future work

In this paper, the novel hybrid ACO-based PID and LuGre friction compensation controlling scheme for 3-DOF high precision flight simulator is designed. On the basis of introduction of the basic principles of ACO, the controlling scheme design for the 3-DOF high precision flight simulator is presented. Based on the popular LuGre friction model, a novel nonlinear friction compensation controller for a kind of 3-DOF high precision flight simulator is developed. The proposed Lyapunov function proves the robust global convergence of the tracking error. The parameters tuning of PID can be summed up as the typical continual spatial optimization problem, grid-based searching strategy is adopted in the improved ACO algorithm, and self-adaptive control strategy for the pheromone decay parameter is also adopted. Modularization design is adopted in the 3-DOF high precision flight simulator. This software can process the position and status signals, and display them on the friendly interface. Double buffer mechanism is adopted in the communication protocol between lower IPC and upper IPC. Series of experiments are conducted, and it is found that the proposed controller has good tracking characteristic and high control precision. The whole high precision flight simulator also has strong robustness.

Our future work will focuses on applying the proposed hybrid ACO-based PID and LuGre friction compensation controller to other industry fields, such as robot control, flight control and process control.

Acknowledgements

This work was supported by the Natural Science Foundation of China under Grant #60604009, Aeronautical Science Foundation of China under Grant #2006ZC51039, Beijing NOVA Program Foundation of China under Grant #2007A017, Open Fund of the Provincial Key Laboratory for Information Processing Technology, Suzhou University under Grant #KJS0821, and "New Scientific Star in Blue Sky" Talent Program of Beihang University of China. The authors are grateful to Prof. Shouzhao Sheng for his detailed guidance in this research work, and also show thanks to the anonymous referees for their valuable comments and suggestions that have led to the better presentation of this paper.

References

[1] A. Ptak, K. Foundy, Real-time spacecraft simulation and hardware-in-the-loop testing, in: Proceedings of the Fourth IEEE Real-time Technology and Applications Symposium, 1998, pp. 230–236.
[2] X. Yue, M. Vilathgamuwa, K.J. Tseng, et al., Modeling and robust adaptive control of a three-axis motion simulator, in: Proceedings of the 2001 IEEE Industry Applications Society Annual Meeting, vol. 1, 2001, pp. 553–560.
[3] K.J. Astrom, T. Hagglund, PID Controllers: Theory Design and Tuning, Instrument Society of America, 1995.
[4] H. Hjalmarsson, M. Gevers, S. Gunnarsson, et al, Iterative feedback tuning: theory and applications, IEEE Control Systems Magazine 18 (4) (1998) 26–41.

[5] J.M. Herrero, X. Blasco, M. Martinez, J.V. Salcedo, Optimal PID tuning with genetic algorithms for non-linear process models, in: Proceedings of the 15th World Congress of IFAC, Barcelona, Spain, 2002.
[6] D. Pierre, H. Vincent, A. Brian, et al., Single state elastoplastic friction models, IEEE Transactions on Automatic Control 47 (5) (2002) 787–792.
[7] B. Armstrong-Helouvry, P. Dupont, W.C. Canudas, A survey of models analysis tools and compensation methods for the control of machines with friction, Automatica 30 (7) (1994) 1083–1138.
[8] C. Alberto, M. Dorigo, M. Vittorio, et al., Distributed optimization by ant colonies, in: Proceedings of the First European Conference on Artificial Life, 1991, pp. 134–142.
[9] V. Katja, N. Ann, Colonies of learning automata, IEEE Transactions on Systems Man and Cybernetics-Part B 32 (6) (2002) 772–780.
[10] E. Bonabeau, M. Dorigo, G. Theraulaz, Inspiration for optimization from social insect behavior, Nature 406 (6) (2000) 39–42.
[11] H.B. Duan, Ant Colony Algorithms: Theory and Applications, Science Press, Beijing, 2005.
[12] H.B. Duan, D.B. Wang, X.F. Yu, Grid-based ACO algorithm for parameters tuning of NLPID controller and its application in flight simulator, International Journal of Computational Methods 3 (2) (2006) 163–175.
[13] H.B. Duan, D.B. Wang, X.F. Yu, et al, Research on the parameters optimization of PID controller based on ant colony algorithm, Journal of Wuhan University 37 (5) (2004) 97–100.
[14] Y.L. Tan, Non-linear Observer/Controller Design and Its Application to Friction Compensation, University of California, Los Angeles, 2000, pp. 41–65.
[15] C. Canudas de Wit, H. Olsson, K.J. Astrom, et al, A new model for control of systems with friction, IEEE Transaction on Automatic control 40 (3) (1995) 419–425.
[16] H.B. Duan, D.B. Wang, X.F. Yu, Realization of nonlinear PID with feed-forward controller for 3-DOF flight simulator and hardware-in-loop simulation, Journal of Systems Engineering and Electronics 19 (2) (2008) 342–345.
[17] W.Q. Xiong, P. Wei, A kind of ant colony algorithm for function optimization, in: Proceedings of the First International Conference on Machine Learning and Cybernetics, Beijing, 2002, pp. 552–555.
[18] L. Ma, J. Yao, B.Q. Fan, The application of ant algorithm in traffic assignment, Bulletin of Science and Technology 19 (5) (2003) 377–380.
[19] Y. Wang, J.Y. Xie, An adaptive ant colony optimization algorithm and simulation, Journal of System Simulation 14 (1) (2002) 31–33.
[20] H.B. Duan, D.B. Wang, F.Z. Yao, Design and research of the control system for simulator of fire control system in armed helicopter, Journal of System Simulation 16 (7) (2004) 1567–1670.